

Petrology and metamorphic *P-T* conditions of eclogites from the northern Veporic Unit (Western Carpathians, Slovakia)

MARIAN JANÁK¹, ŠTEFAN MÉRES² and PETER IVAN²

¹Geological Institute, Slovak Academy of Sciences, Dúbravská cesta 9, P.O. Box 106, 840 05 Bratislava 45, Slovak Republic; marian.janak@savba.sk

²Department of Geochemistry, Faculty of Natural Sciences, Comenius University, Mlynská dolina G, 842 15 Bratislava, Slovak Republic

(Manuscript received May 25, 2006; accepted in revised form October 10, 2006)

Abstract: Eclogites with rarely preserved peak metamorphic assemblage omphacite + garnet + phengite + rutile + zoisite + quartz ± amphibole are present in the northern parts of the Veporic Unit, in the Central Western Carpathians of Slovakia. Retrogression led to breakdown of primary phases. Apart from inclusions in the garnet, primary omphacite (Cpx I) has been converted to symplectites of clinopyroxene with lower Na and Al content (Cpx II) and sodic plagioclase. This resulted from the decompression to the high-pressure granulite facies stability field. Several generations of amphibole (pargasite, hornblende, and actinolite) are evidence of a transformation down to amphibolite and even greenschist facies conditions. Geothermobarometry on the eclogite facies mineral assemblage garnet + omphacite + quartz + phengite allowed us to constrain the maximum pressure and temperature conditions of around 2.5 GPa and 700 °C, implying initial subduction to depths of around 80 km. Our study supports previous indications on the existence of eclogites in the Western Carpathians; careful observations can discover high-pressure phases in potential eclogite-facies rocks. This can be essential to regional correlations and elucidation of the tectonometamorphic evolution of the Western Carpathians during the Variscan orogeny.

Key words: Western Carpathians, retrogression, high-pressure metamorphism, omphacite, eclogite.

Introduction

High-pressure, true eclogite facies rocks have previously been unknown in the Western Carpathians (e.g. Krist et al. 1992; Bezák et al. 1993). In recent years, relics of eclogite facies metamorphism have been inferred in some garnet- and clinopyroxene-bearing metabasites of the basement of the Central Western Carpathians. In these rocks a high-pressure stage has been deduced from textures as symplectites, kelyphites and coronas, indicating a breakdown of primary omphacite (e.g. Hovorka & Méres 1989; Janák et al. 1997 and references therein).

The pre-Tertiary complexes of the Central Western Carpathians comprise six principal superunits: the Tatric, Veporic and Gemeric thick-skinned basement/cover sheets, and the Fatric, Hronic and Silicic detachment cover nappe systems (Plašienka et al. 1997). Presumed eclogites have been described from several so-called “core mountains”: Tribeč (Hovorka & Méres 1990), Malá Fatra (Hovorka et al. 1992a; Janák & Lupták 1997; Korikovsky & Hovorka 2001), Western Tatra (Janák et al. 1996) and Low Tatra (Spišiak & Pitoňák 1990), all belonging to the Tatric Unit. Moreover, high-density nitrogen inclusions identical to those observed in well-preserved eclogites of the world have been identified in the metabasites of the Western Tatra (Janák et al. 1996; Hurai et al. 2000). Finally, omphacite has been discovered in metabasites of the northern Veporic Unit (Janák et al. 2003).

Following the first report (Janák et al. 2003), we present here more in detail the mineralogical and petrologic features of eclogites from the northern Veporic Unit in the

Central Western Carpathians. The microtextures, mineral assemblages and their compositions, which constrain the high-pressure eclogite stage and subsequent retrogression during decompression are described. The peak metamorphism, eclogite facies stage *P-T* conditions are evaluated by thermobarometry. We propose that the formation of eclogites resulted from subduction, most probably during the Variscan orogeny. However, resolving their initial setting and protolith are beyond the scope of this paper.

Geological background

The investigated eclogites occur in the northern parts of the Veporic Unit (Fig. 1). The Veporic Unit consists of pre-Alpine basement that is overlain by the Upper Paleozoic–Triassic sedimentary cover. The magmatic and metamorphic history of the Veporic Unit was polyphase, comprising the pre-Variscan, Variscan, Permian and Alpine events (e.g. Plašienka et al. 1997 and references therein).

The northern parts of the Veporic Unit are composed of several basement complexes covered by Permian and Mesozoic rocks (Fig. 1). The eclogites are part of the basement termed the Hron Complex (Klinec 1966), leptyno-amphibolite complex (Hovorka et al. 1992b, 1994, 1997) or layered metaigneous complex (Putiš et al. 1997). In this paper we use the term “leptyno-amphibolite complex” (LAC). In the investigated area, LAC is composed of several rock types. The most abundant are amphibolites and gneisses (both ortho- and para-gneisses). These are strongly deformed and retrogressed to epidote amphibolites, micaschists and phyl-

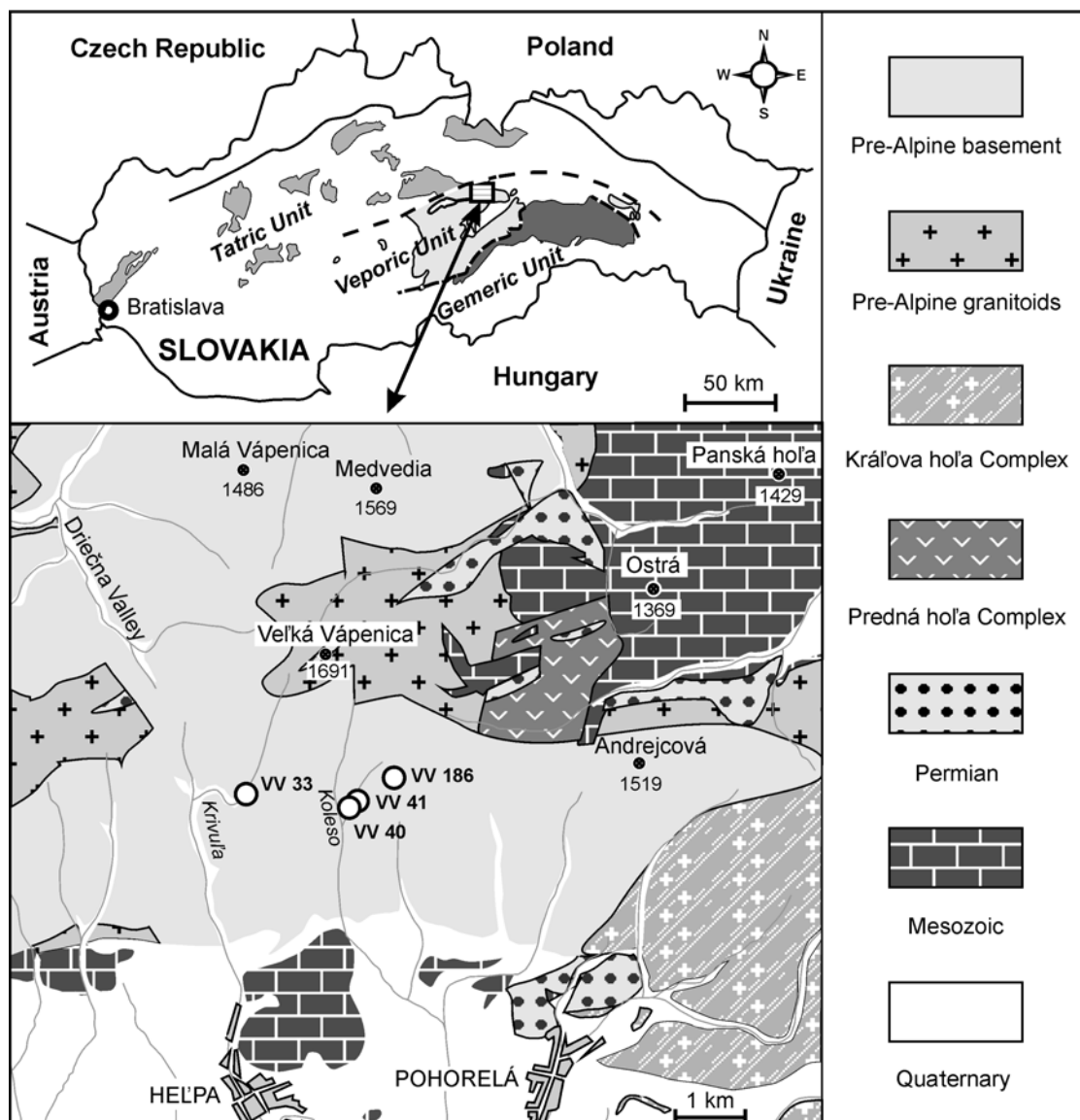


Fig. 1. Simplified geological map of the northern parts of the Veporic Unit modified from Biely et al. (1992) showing locations of the investigated eclogites.

lites. Within these rocks, massive metaultramafites, metagabbros and garnet-clinopyroxene amphibolites occur as blocks and lenses of meter to tens of meters size. The metagabbros have partly well-preserved their primary cumulate texture and minerals (Ivan et al. 1996; Méres et al. 1996; Putiš et al. 1997). Less metamorphosed rocks within this complex (phyllites, metasandstones, mafic volcanics and volcanoclastics) have been distinguished as Jánov grúň Complex (Miko 1981) of probably Permian age (Kotov et al. 1996). In the investigated area these rocks are considered to be diaphthorites of LAC amphibolites and therefore not shown on the map. Pre-Alpine granitoids together with associated gneisses and micaschists strongly affected by Alpine mylonitization belong to the Kráľova hoľa Complex. The intrusion age of these granitoids is 350 Ma according to SHRIMP dating of zircons (Gaab et al. 2006b). The Predná hoľa Complex is composed of Paleozoic, low-grade

metamorphosed phyllites, metasandstones, basic volcanics and volcanoclastics. Permian rocks comprise metamorphosed conglomerates, sandstones, arkoses and greywackes locally with volcanogenic material. Mesozoic rocks consist of Triassic carbonates and quartzites affected by low-grade metamorphism in the Cretaceous time (Vrána 1966; Korikovsky et al. 1997; Lupták et al. 2003).

Petrography and mineral chemistry

The investigated eclogites have been found in the outcrops in the Koleso and Krivúľa Valleys north of Hel'pa (Fig. 1). The eclogites occur mostly as lenses and boudins within amphibolites; the best-preserved forming the cores of such lenses. Reddish garnet and pale green clinopyroxene are variably replaced by amphibole (Fig. 2a,b). Micro-

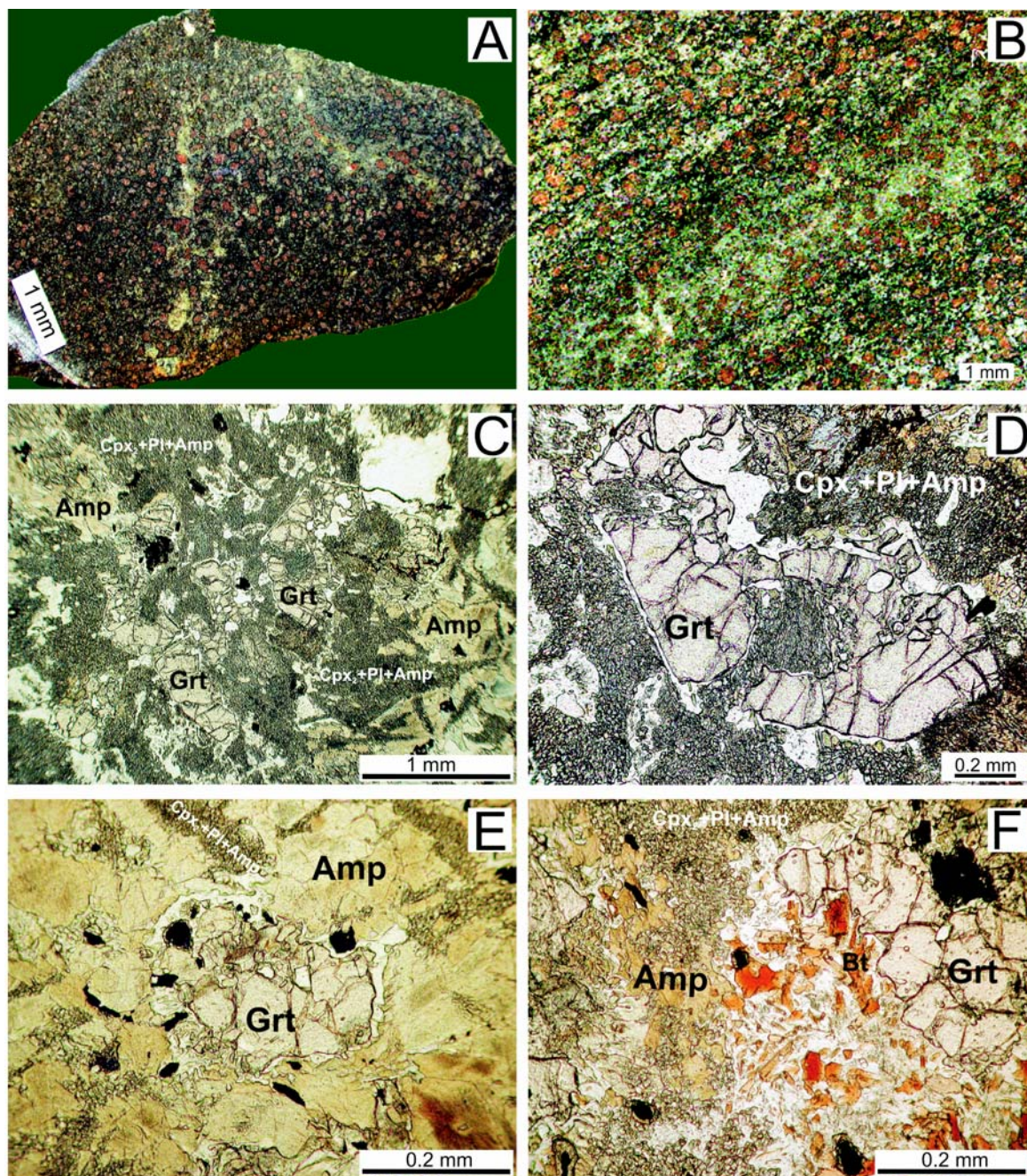


Fig. 2. Textures of the investigated eclogites. **a** — Photograph of relatively well-preserved eclogite in sample VV 40. **b** — Detail of texture with reddish garnet and pale green clinopyroxene variably replaced by amphibole in sample VV 33. **c–f** — Photomicrographs of the eclogite facies minerals breakdown. **c,d** — Garnet porphyroblasts surrounded and partly resorbed by clinopyroxene-plagioclase-amphibole symplectites, larger amphiboles are at a distance from the garnet contacts. Sample VV 33, plane-polarized light. **e** — More advanced stage of retrogression with large pleochroic, green to brown-green amphiboles replacing garnet in VV 33, plane-polarized light. **f** — Symplectite of red-brown biotite with plagioclase and quartz (white) after phengite. Sample VV 41, plane-polarized light.

structures along with variations in mineral chemistry suggest that the rocks have experienced a multistage metamorphic history. The composition of main mineral phases was determined using a CAMECA SX-100 electron microprobe at the State Geological Institute of Dionýz Štúr in Bratislava. The analytical conditions were 15 kV accelerating voltage and 20 nA beam current, with a peak counting time of 20 seconds and a beam diameter of 2–10 μm . Raw counts

were corrected using a PAP routine. Mineral abbreviations are according to Kretz (1983).

Garnet

Garnet is poikiloblastic with inclusions of clinopyroxene, amphibole, quartz, zoisite and rutile/ilmenite. It is surrounded and partly resorbed by clinopyroxene-pla-

gioclase-amphibole symplectites (Figs. 2c,d and 3a), and amphibole-plagioclase kelyphites (Fig. 2e,f). The composition of garnet (Table 1) shows a large range of almandine (52–62 mol %), pyrope (6–20 mol %), grossular (27–40 mol %) and spessartine (1–2 mol %) end mem-

bers. The compositional profiles in the individual grains (Figs. 3c and 5) are very smooth, showing steady Mg increase concomitant with Fe and Fe/Fe+Mg decrease from the core to the rim, at nearly constant Ca, which is characteristic for a prograde growth zoning. The maximum Mg

Table 1: Representative analyses of garnet. Formula normalization to 12 oxygens and 8 cations, Fe³⁺ by charge balance.

| Sample | VV41 | VV41 | VV41 | VV40 | VV40 | VV40 | VV33 | VV33 | VV33 | VV186 | VV186 |
|--------------------------------|--------|--------|--------|--------|-------|-------|-------|--------|-------|--------|--------|
| Point | core | rim* | edge | core | rim* | edge | core | rim* | edge | core | rim* |
| SiO ₂ | 37.79 | 37.68 | 38.10 | 38.50 | 38.64 | 38.50 | 38.50 | 38.62 | 38.26 | 37.52 | 37.54 |
| TiO ₂ | 0.00 | 0.23 | 0.10 | 0.19 | 0.04 | 0.04 | 0.20 | 0.18 | 0.11 | 0.19 | 0.06 |
| Al ₂ O ₃ | 21.39 | 21.33 | 21.32 | 21.61 | 21.67 | 21.33 | 21.00 | 21.52 | 20.99 | 21.38 | 21.30 |
| Cr ₂ O ₃ | 0.00 | 0.05 | 0.04 | 0.04 | 0.02 | 0.00 | 0.01 | 0.02 | 0.02 | 0.02 | 0.20 |
| FeO | 27.95 | 26.35 | 23.98 | 25.33 | 24.09 | 25.26 | 25.10 | 24.79 | 25.16 | 26.59 | 25.70 |
| MnO | 1.03 | 0.47 | 0.57 | 0.68 | 0.34 | 0.64 | 0.76 | 0.51 | 0.71 | 0.64 | 0.39 |
| MgO | 1.61 | 2.11 | 1.57 | 3.96 | 5.23 | 4.14 | 4.29 | 4.33 | 4.11 | 2.15 | 2.06 |
| CaO | 10.29 | 12.52 | 14.42 | 10.24 | 9.88 | 9.77 | 9.91 | 10.32 | 10.04 | 11.84 | 13.01 |
| Total | 100.06 | 100.74 | 100.10 | 100.55 | 99.91 | 99.68 | 99.77 | 100.29 | 99.40 | 100.33 | 100.26 |
| Si | 3.00 | 2.95 | 2.998 | 3.00 | 3.00 | 3.02 | 3.02 | 3.00 | 3.01 | 2.96 | 2.95 |
| Ti | 0.00 | 0.01 | 0.006 | 0.01 | 0.00 | 0.00 | 0.01 | 0.01 | 0.01 | 0.01 | 0.00 |
| Al | 2.00 | 1.97 | 1.978 | 1.98 | 1.98 | 1.97 | 1.94 | 1.97 | 1.95 | 1.99 | 1.98 |
| Cr | 0.00 | 0.00 | 0.002 | 0.00 | 0.00 | 0.00 | 0.00 | 0.00 | 0.00 | 0.00 | 0.01 |
| Fe ³⁺ | 0.00 | 0.09 | 0.012 | 0.00 | 0.01 | 0.00 | 0.02 | 0.01 | 0.02 | 0.08 | 0.10 |
| Fe ²⁺ | 1.86 | 1.64 | 1.566 | 1.65 | 1.55 | 1.66 | 1.63 | 1.61 | 1.63 | 1.67 | 1.59 |
| Mn | 0.07 | 0.03 | 0.038 | 0.05 | 0.02 | 0.04 | 0.05 | 0.03 | 0.05 | 0.04 | 0.03 |
| Mg | 0.19 | 0.25 | 0.184 | 0.46 | 0.61 | 0.48 | 0.50 | 0.50 | 0.48 | 0.25 | 0.24 |
| Ca | 0.88 | 1.05 | 1.217 | 0.86 | 0.82 | 0.82 | 0.83 | 0.86 | 0.85 | 1.00 | 1.10 |
| Total | 8.00 | 8.00 | 8.00 | 8.00 | 8.00 | 7.99 | 7.99 | 8.00 | 8.00 | 8.00 | 8.00 |
| X _{alm} | 0.62 | 0.55 | 0.52 | 0.55 | 0.52 | 0.55 | 0.54 | 0.53 | 0.54 | 0.56 | 0.54 |
| X _{sps} | 0.02 | 0.01 | 0.01 | 0.01 | 0.01 | 0.01 | 0.02 | 0.01 | 0.02 | 0.01 | 0.01 |
| X _{prp} | 0.06 | 0.08 | 0.06 | 0.15 | 0.20 | 0.16 | 0.17 | 0.17 | 0.16 | 0.08 | 0.08 |
| X _{grs} | 0.29 | 0.35 | 0.40 | 0.28 | 0.27 | 0.27 | 0.28 | 0.29 | 0.28 | 0.34 | 0.37 |

*garnet with maximum (a_{grs})² · (a_{py}) used for *P-T* calculations

Table 2: Representative analyses of clinopyroxene. Formula normalization to 6 oxygens and 4 cations, Fe³⁺ by charge balance.

| Sample | VV41 | VV41 | VV41 | VV41 | VV40 | VV40 | VV40 | VV40 | VV33 | VV33 | VV33 | VV33 | VV186 | VV186 | VV186 | VV186 |
|--------------------------------|--------|--------|--------|--------|--------|--------|--------|--------|--------|--------|--------|--------|-------|--------|--------|--------|
| Type | Cpx I | Cpx I | Cpx I | Cpx II | Cpx I | Cpx I | Cpx I | Cpx II | Cpx I | Cpx I | Cpx I | Cpx II | Cpx I | Cpx I | Cpx I | Cpx II |
| SiO ₂ | 54.92 | 54.84 | 54.66 | 52.28 | 54.58 | 54.43 | 54.90 | 53.92 | 55.28 | 54.85 | 54.70 | 53.28 | 54.12 | 53.57 | 54.96 | 52.31 |
| TiO ₂ | 0.09 | 0.09 | 0.09 | 0.06 | 0.13 | 0.11 | 0.09 | 0.07 | 0.08 | 0.08 | 0.14 | 0.07 | 0.12 | 0.13 | 0.10 | 0.03 |
| Al ₂ O ₃ | 10.93 | 9.78 | 9.43 | 0.81 | 7.80 | 7.75 | 8.68 | 1.93 | 9.16 | 8.50 | 8.39 | 1.32 | 10.51 | 8.90 | 9.62 | 0.98 |
| Cr ₂ O ₃ | 0.00 | 0.00 | 0.00 | 0.29 | 0.00 | 0.04 | 0.06 | 0.11 | 0.00 | 0.03 | 0.02 | 0.07 | 0.00 | 0.00 | 0.31 | 0.20 |
| FeO | 8.13 | 8.71 | 8.60 | 13.71 | 5.78 | 7.23 | 5.96 | 7.02 | 6.65 | 6.10 | 6.20 | 7.35 | 7.70 | 7.99 | 7.54 | 12.89 |
| MnO | 0.01 | 0.06 | 0.06 | 0.10 | 0.02 | 0.01 | 0.06 | 0.10 | 0.11 | 0.03 | 0.05 | 0.09 | 0.06 | 0.09 | 0.07 | 0.06 |
| MgO | 6.57 | 6.88 | 7.30 | 10.04 | 10.40 | 9.67 | 10.07 | 13.46 | 9.18 | 9.86 | 9.80 | 14.04 | 7.11 | 8.51 | 8.05 | 10.72 |
| CaO | 14.24 | 14.21 | 14.72 | 22.08 | 17.18 | 17.09 | 17.11 | 23.00 | 15.19 | 16.77 | 16.41 | 23.84 | 14.05 | 16.38 | 15.41 | 22.35 |
| Na ₂ O | 5.89 | 5.73 | 5.50 | 0.70 | 4.14 | 4.38 | 3.96 | 0.97 | 5.28 | 4.64 | 4.95 | 0.54 | 5.61 | 4.56 | 5.23 | 0.57 |
| K ₂ O | 0.01 | 0.00 | 0.00 | 0.00 | 0.00 | 0.00 | 0.00 | 0.00 | 0.01 | 0.00 | 0.00 | 0.00 | 0.01 | 0.00 | 0.00 | 0.00 |
| Total | 100.79 | 100.32 | 100.43 | 100.13 | 100.05 | 100.89 | 100.89 | 100.64 | 101.03 | 100.99 | 100.91 | 100.79 | 99.29 | 100.27 | 101.30 | 100.19 |
| Si | 1.98 | 1.99 | 1.98 | 1.99 | 1.97 | 1.96 | 1.97 | 1.98 | 1.97 | 1.96 | 1.96 | 1.96 | 1.97 | 1.95 | 1.97 | 1.98 |
| Ti | 0.00 | 0.00 | 0.00 | 0.00 | 0.00 | 0.00 | 0.00 | 0.00 | 0.00 | 0.00 | 0.00 | 0.00 | 0.00 | 0.00 | 0.00 | 0.00 |
| Al | 0.46 | 0.42 | 0.40 | 0.04 | 0.33 | 0.33 | 0.37 | 0.08 | 0.39 | 0.36 | 0.35 | 0.06 | 0.45 | 0.38 | 0.41 | 0.04 |
| Cr | 0.00 | 0.00 | 0.00 | 0.01 | 0.00 | 0.00 | 0.00 | 0.00 | 0.00 | 0.00 | 0.00 | 0.00 | 0.00 | 0.00 | 0.01 | 0.01 |
| Fe ³⁺ | 0.00 | 0.01 | 0.02 | 0.02 | 0.01 | 0.05 | 0.00 | 0.02 | 0.03 | 0.03 | 0.07 | 0.05 | 0.00 | 0.04 | 0.00 | 0.02 |
| Fe ²⁺ | 0.24 | 0.26 | 0.24 | 0.42 | 0.17 | 0.17 | 0.18 | 0.20 | 0.17 | 0.15 | 0.12 | 0.17 | 0.24 | 0.21 | 0.22 | 0.39 |
| Mn | 0.00 | 0.00 | 0.00 | 0.00 | 0.00 | 0.00 | 0.00 | 0.00 | 0.00 | 0.00 | 0.00 | 0.00 | 0.00 | 0.00 | 0.00 | 0.00 |
| Mg | 0.35 | 0.37 | 0.39 | 0.57 | 0.56 | 0.52 | 0.54 | 0.74 | 0.49 | 0.53 | 0.52 | 0.77 | 0.39 | 0.46 | 0.43 | 0.61 |
| Ca | 0.55 | 0.55 | 0.57 | 0.90 | 0.67 | 0.66 | 0.66 | 0.91 | 0.58 | 0.64 | 0.63 | 0.94 | 0.55 | 0.64 | 0.59 | 0.91 |
| Na | 0.41 | 0.40 | 0.39 | 0.05 | 0.29 | 0.31 | 0.28 | 0.07 | 0.37 | 0.32 | 0.34 | 0.04 | 0.40 | 0.32 | 0.36 | 0.04 |
| K | 0.00 | 0.00 | 0.00 | 0.00 | 0.00 | 0.00 | 0.00 | 0.00 | 0.00 | 0.00 | 0.00 | 0.00 | 0.00 | 0.00 | 0.00 | 0.00 |
| Total | 4.00 | 4.00 | 4.00 | 4.00 | 4.00 | 4.00 | 3.98 | 4.00 | 4.00 | 4.00 | 4.00 | 4.00 | 4.00 | 4.00 | 4.00 | 4.00 |
| X _{jd} | 0.41 | 0.39 | 0.37 | 0.03 | 0.28 | 0.26 | 0.27 | 0.05 | 0.34 | 0.29 | 0.27 | 0.00 | 0.39 | 0.28 | 0.35 | 0.02 |

and the lowest Fe/Fe+Mg occur close to the rim. In the outermost part of the rims, Mn, Fe and Fe/Fe+Mg rise whereas Mg drops as a result of resorption due to retrogression.

Clinopyroxene

Primary clinopyroxene (Cpx I) — omphacite occurs as inclusions in garnet, attaining the size of mostly less than 10

micrometers (Fig. 3a,b) but larger omphacite of several tens of micrometers can also be observed (Figs. 3d and 4a-c). The composition of omphacite varies between individual samples but also within grains (Table 2). The jadeite content shows a wide range from 26–29 mol % to 39–41 mol %. Differences in the Mg/Fe ratio are most probably due to bulk chemistry as reflected also by other minerals. Breakdown of omphacite led to the formation of less jadei-

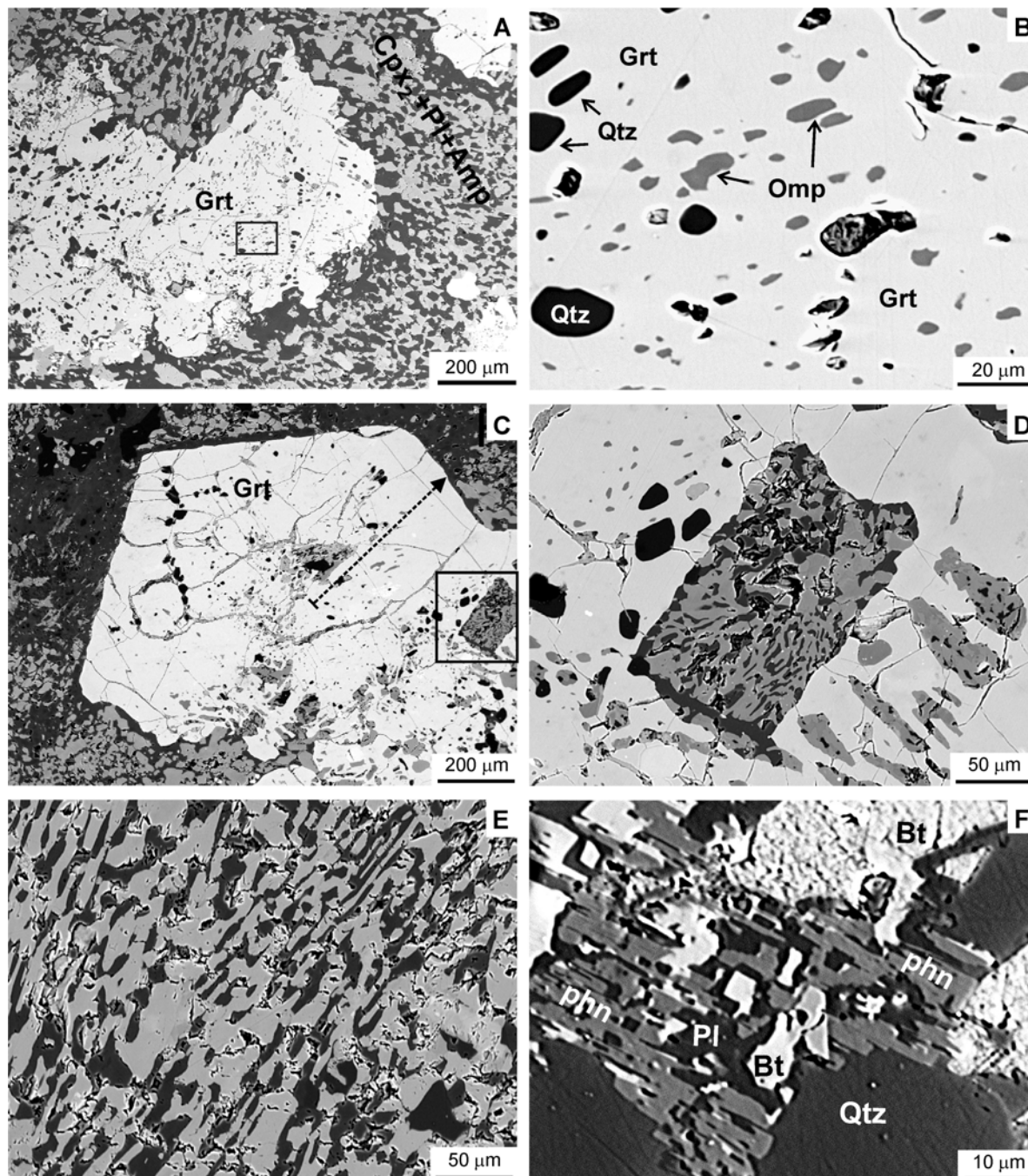


Fig. 3. Back-scattered electron (BSE) images. **a–d** — Garnet porphyroblasts with inclusions of primary clinopyroxene — omphacite. **a,b** — Minor inclusions of pristine omphacite in sample VV 41. **c,d** — Breakdown of larger omphacite to symplectite of Cpx II (light grey) and plagioclase (black) in sample VV 40. The arrow in garnet marks the position of the compositional profile shown on Fig. 5. **e** — BSE image showing symplectites of clinopyroxene II (light grey), amphibole (dark grey) and plagioclase (black) in sample VV 186. **f** — BSE image of phengite partially replaced by symplectite of biotite and plagioclase in sample VV 186.

te-rich Cpx II, which forms symplectitic intergrowths with Na-rich plagioclase (Figs. 3d,e and 4c-e). Amphibole is also common in these symplectites but appears to be a later phase replacing the pyroxene. The secondary Cpx II has a lower Na and higher Ca but a similar Fe content to primary Cpx I during this transformation, as documented by compositional maps of these elements (Fig. 4d-f).

Phengite

Phengite commonly associated with quartz occurs in the matrix. Mineral compositions show a wide range in Mg/Fe

ratio and up to 3.4 Si p.f.u (Table 3). Breakdown of phengite led to the formation of biotite and plagioclase which form the symplectitic intergrowths (Figs. 2f and 3f).

Amphibole

Amphibole occurs as several compositional and textural types. Amphibole inclusions in garnet (Amp I) form small euhedral crystals, and are classified as hornblende to pargasite. Amphibole II of pargasitic composition can be recognized in kelyphitic rims around garnets as lath-shaped crystals, or symplectitic intergrowths with clinopyroxene

Table 3: Representative analyses of phengite. Formula normalization to 11 oxygens.

| Sample | VV41 | VV41 | VV40 | VV40 | VV33 | VV33 | VV186 | VV186 |
|--------------------------------|-------|-------|-------|-------|-------|-------|-------|-------|
| SiO ₂ | 49.91 | 48.10 | 49.39 | 49.62 | 50.53 | 50.26 | 51.08 | 50.79 |
| TiO ₂ | 0.29 | 0.14 | 0.13 | 0.16 | 0.02 | 0.02 | 0.50 | 0.45 |
| Al ₂ O ₃ | 30.37 | 29.88 | 30.00 | 29.25 | 30.47 | 29.91 | 27.88 | 27.44 |
| Cr ₂ O ₃ | 0.04 | 0.03 | 0.00 | 0.16 | 0.00 | 0.00 | 0.10 | 0.03 |
| FeO | 2.97 | 2.82 | 2.08 | 2.81 | 2.03 | 1.84 | 2.07 | 1.68 |
| MnO | 0.00 | 0.06 | 0.00 | 0.00 | 0.00 | 0.03 | 0.00 | 0.00 |
| MgO | 2.49 | 2.44 | 3.63 | 3.84 | 2.78 | 2.85 | 2.81 | 3.17 |
| CaO | 0.10 | 0.03 | 0.04 | 0.07 | 0.09 | 0.08 | 0.07 | 0.03 |
| Na ₂ O | 0.37 | 0.22 | 0.14 | 0.14 | 0.32 | 0.11 | 0.23 | 0.23 |
| K ₂ O | 10.35 | 10.99 | 10.27 | 10.43 | 10.37 | 10.73 | 10.53 | 10.78 |
| Total | 96.89 | 94.71 | 95.68 | 96.48 | 96.61 | 95.83 | 95.27 | 94.60 |
| Si | 3.28 | 3.25 | 3.27 | 3.28 | 3.31 | 3.33 | 3.40 | 3.41 |
| Ti | 0.01 | 0.01 | 0.01 | 0.01 | 0.00 | 0.00 | 0.03 | 0.02 |
| Al | 2.35 | 2.38 | 2.34 | 2.28 | 2.35 | 2.33 | 2.19 | 2.17 |
| Cr | 0.00 | 0.00 | 0.00 | 0.01 | 0.00 | 0.00 | 0.01 | 0.00 |
| Fe | 0.16 | 0.16 | 0.11 | 0.15 | 0.11 | 0.10 | 0.12 | 0.09 |
| Mn | 0.00 | 0.00 | 0.00 | 0.00 | 0.00 | 0.00 | 0.00 | 0.00 |
| Mg | 0.24 | 0.25 | 0.36 | 0.38 | 0.27 | 0.28 | 0.28 | 0.32 |
| Ca | 0.01 | 0.00 | 0.00 | 0.00 | 0.01 | 0.01 | 0.01 | 0.00 |
| Na | 0.05 | 0.03 | 0.02 | 0.02 | 0.04 | 0.01 | 0.03 | 0.03 |
| K | 0.87 | 0.95 | 0.87 | 0.88 | 0.87 | 0.91 | 0.90 | 0.92 |
| Total | 6.97 | 7.03 | 6.97 | 7.00 | 6.96 | 6.97 | 6.94 | 6.97 |

Table 4: Representative analyses of amphibole. Formula normalization to 23 oxygens, Fe³⁺ as average from minimum and maximum constraints.

| Sample | VV41 | VV41 | VV41 | VV40 | VV40 | VV40 | VV33 | VV33 | VV186 | VV186 |
|--------------------------------|-------|---------|--------|-------|--------|---------|--------|---------|-------|--------|
| Type | Amp I | Amp III | Amp IV | Amp I | Amp II | Amp III | Amp II | Amp III | Amp I | Amp II |
| SiO ₂ | 41.95 | 41.59 | 52.95 | 46.48 | 44.73 | 48.17 | 42.82 | 49.86 | 41.72 | 46.92 |
| TiO ₂ | 0.49 | 1.20 | 0.05 | 0.74 | 1.59 | 1.20 | 1.18 | 0.95 | 1.22 | 0.21 |
| Al ₂ O ₃ | 15.45 | 13.11 | 1.68 | 11.60 | 12.10 | 8.56 | 13.90 | 7.16 | 13.02 | 9.06 |
| Cr ₂ O ₃ | 0.06 | 0.64 | 0.02 | 0.09 | 0.27 | 0.08 | 0.03 | 0.16 | 0.02 | 0.20 |
| FeO | 15.50 | 19.53 | 19.71 | 12.02 | 13.03 | 11.39 | 13.14 | 10.37 | 16.94 | 18.05 |
| MnO | 0.06 | 0.07 | 0.15 | 0.04 | 0.09 | 0.07 | 0.09 | 0.09 | 0.06 | 0.07 |
| MgO | 9.60 | 7.05 | 10.69 | 13.47 | 12.14 | 14.31 | 11.11 | 15.80 | 9.21 | 9.83 |
| CaO | 11.28 | 11.12 | 12.23 | 11.82 | 11.89 | 11.89 | 12.14 | 11.83 | 11.46 | 11.92 |
| Na ₂ O | 2.62 | 2.35 | 0.17 | 1.56 | 1.71 | 1.28 | 2.09 | 1.11 | 2.07 | 1.10 |
| K ₂ O | 0.43 | 0.83 | 0.12 | 0.60 | 0.84 | 0.55 | 0.57 | 0.25 | 1.15 | 0.53 |
| Total | 97.44 | 97.49 | 97.77 | 98.42 | 98.39 | 97.50 | 97.07 | 97.58 | 96.87 | 97.89 |
| Si | 6.23 | 6.34 | 7.86 | 6.68 | 6.51 | 6.97 | 6.35 | 7.12 | 6.33 | 6.97 |
| Ti | 0.06 | 0.14 | 0.01 | 0.08 | 0.17 | 0.13 | 0.13 | 0.10 | 0.14 | 0.02 |
| Al | 2.71 | 2.36 | 0.29 | 1.96 | 2.08 | 1.46 | 2.43 | 1.21 | 2.33 | 1.59 |
| Cr | 0.01 | 0.08 | 0.00 | 0.01 | 0.03 | 0.01 | 0.00 | 0.02 | 0.00 | 0.02 |
| Fe ³⁺ | 0.19 | 0.07 | 0.00 | 0.21 | 0.11 | 0.12 | 0.03 | 0.22 | 0.12 | 0.12 |
| Fe ²⁺ | 1.74 | 2.42 | 2.45 | 1.23 | 1.48 | 1.25 | 1.60 | 1.02 | 2.03 | 2.12 |
| Mn | 0.01 | 0.01 | 0.02 | 0.01 | 0.01 | 0.01 | 0.01 | 0.01 | 0.01 | 0.01 |
| Mg | 2.13 | 1.60 | 2.37 | 2.88 | 2.64 | 3.08 | 2.46 | 3.36 | 2.08 | 2.18 |
| Ca | 1.80 | 1.82 | 1.95 | 1.82 | 1.86 | 1.84 | 1.93 | 1.81 | 1.86 | 1.90 |
| Na | 0.75 | 0.70 | 0.05 | 0.43 | 0.48 | 0.36 | 0.60 | 0.31 | 0.61 | 0.32 |
| K | 0.08 | 0.16 | 0.02 | 0.11 | 0.16 | 0.10 | 0.11 | 0.05 | 0.22 | 0.10 |
| Total | 15.69 | 15.70 | 15.02 | 15.42 | 15.52 | 15.34 | 15.65 | 15.23 | 15.73 | 15.35 |

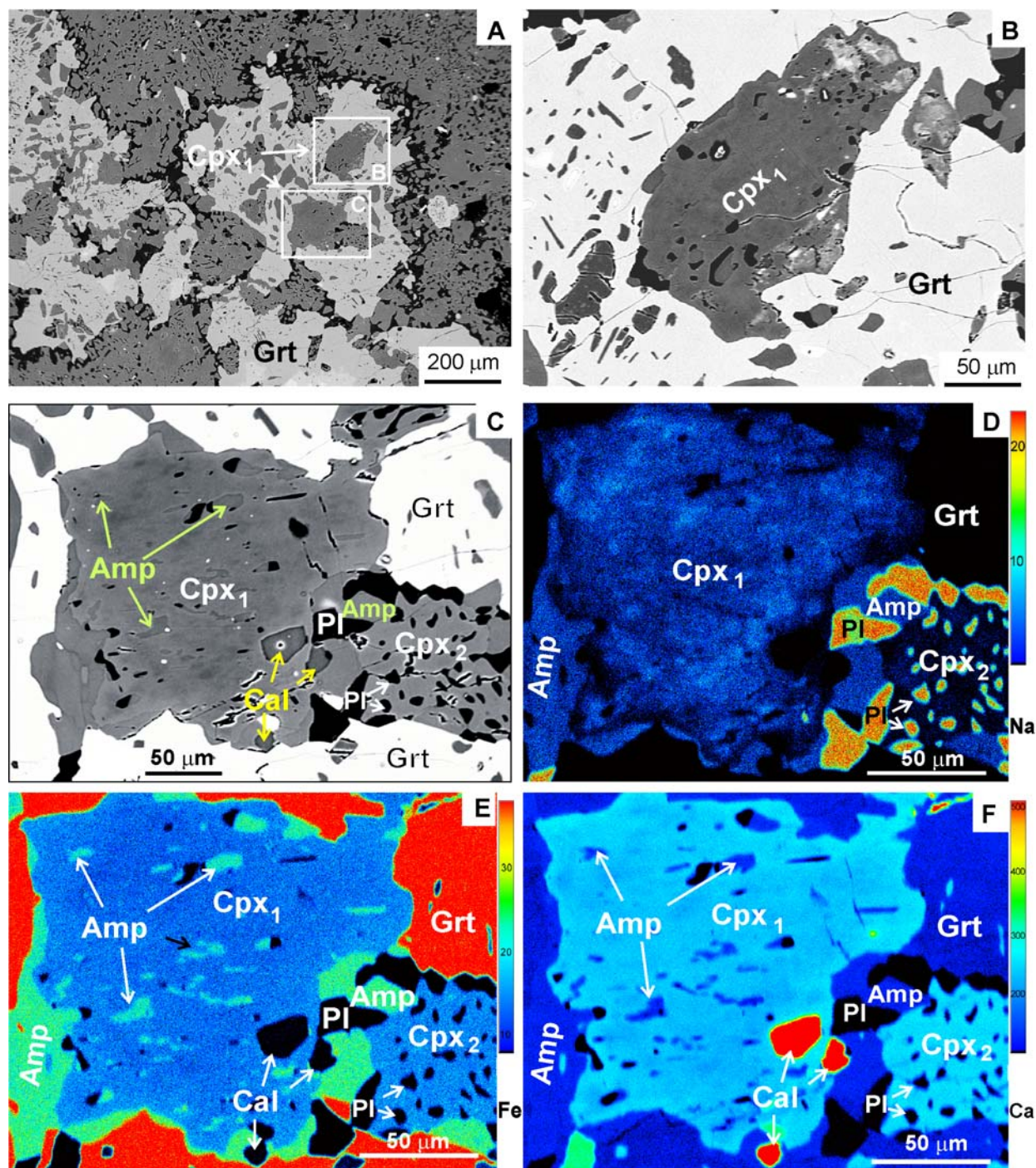


Fig. 4. BSE images and compositional X-ray maps of the omphacite breakdown. **a** — BSE image of omphacite inclusions in garnet, sample VV 33. **b** — Detail of omphacite. **c** — Breakdown of primary Cpx I (omphacite) to Cpx II, plagioclase, amphibole and calcite as retrograde phases. **d–f** — Quantitative X-ray maps of area in (c) showing Na, Fe and Ca distribution. Note that complex compositional zonation with highest Na in (d) and lowest Ca in (f) is seen within the Cpx I domain.

and plagioclase (Figs. 2c–f, 3a,e and 4c–e). Matrix amphiboles (Amp III) at a distance from the garnet contacts are relatively large, pleochroic, dark green to brown-green poikiloblastic grains, of hornblende to pargasite composition. Actinolite (Amp IV) is a later phase that formed around earlier amphiboles. The compositions of amphiboles are presented in Table 4.

Minor phases

Zoisite is common as inclusions in garnet porphyroblasts and it is considered to be a part of the eclogite facies assemblage. Epidote (clinozoisite) is present in the matrix where it is commonly associated with amphibole as retrograde phases. Plagioclase occurs only as a secondary

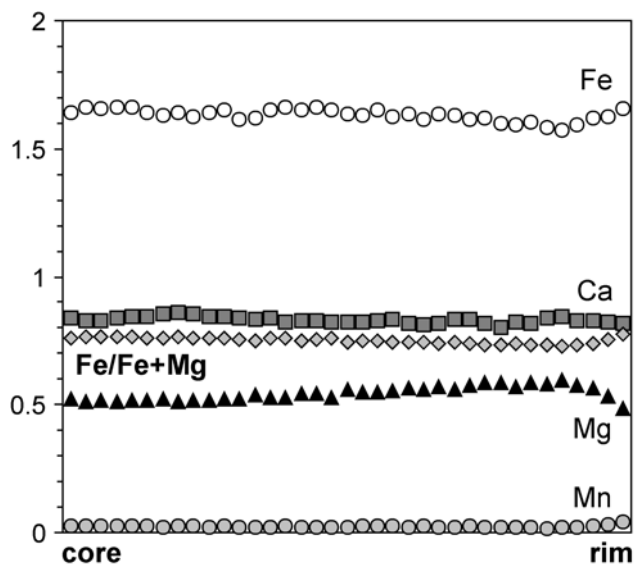
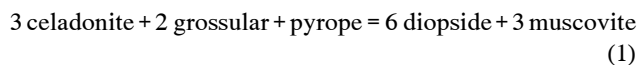


Fig. 5. Compositional profile of garnet in sample VV 40. The position of line is shown on Fig. 3c.

mineral, forming symplectites with Cpx II and biotite after omphacite and phengite. Plagioclase is also present in the kelyphitic rims around garnet. K-feldspar is a minor phase found as inclusion in garnet. Quartz occurs in garnet, in kelyphites, and in the matrix. Rutile and ilmenite are ubiquitous as inclusions in garnet, matrix amphibole, and kelyphites. Sphene is abundant in the most retrograded domains and biotite; chlorite and calcite have been recognized as additional retrograde minerals.

Geothermobarometry

Peak metamorphic conditions have been calculated from geothermobarometry on the eclogite facies mineral assemblage garnet+omphacite+phengite. A combination of the garnet-clinopyroxene Fe^{2+} -Mg exchange geothermometer of Ravna (2000) with the geobarometer utilizing the net-transfer reaction equilibrium:



calibrated by Ravna & Terry (2004) has been used. A combination of the activity model for the phengite solid solution by Holland & Powell (1998), the clinopyroxene activity model of Holland (1990), and the garnet activity model of Ganguly et al. (1996) were selected as recommended by Ravna & Terry (2004). We used omphacite with the highest jadeite content, garnet with maximum $(a_{\text{grs}})^2 \cdot (a_{\text{py}})$ and phengite with the highest Si content to calculate maximum pressure conditions. For garnet-omphacite geothermometry the ferric Fe in garnet and omphacite was calculated from the stoichiometry. In the omphacite, we have also calculated the ferric Fe contents following the procedure, which only allocates Fe^{3+} if there is excess Na over the content of Al present.

The intersection values of garnet-clinopyroxene thermometer with equilibrium (1) in four investigated samples are presented in Table 5. They yield a pressure of 2.3–2.7 GPa and temperature in the range of 684–725 °C. These pressure and temperature values correspond well to the stability field of eclogite facies metamorphism (Fig. 6). The spread in temperature and pressure can be attributed to the post-eclogite facies reequilibration during decompression and exhumation. Post peak metamorphic overprint may cause partial redistribution of Fe and Mg between garnet and clinopyroxene. Uncertainty related to the oxidation state of iron can be an additional problem concerning the estimation of temperature. According to Ravna & Paquin (2003), the uncertainty of garnet-clinopyroxene thermometer may be ± 60 °C. The garnet-clinopyroxene-phengite barometer applied here may give invariably higher pressures than the original calibration of Waters & Martin (1993, 1996) or its other applications (e.g. Carswell et al. 1997). Except different barometric expressions this stems largely from the preferred garnet activity model used. Nevertheless, it can be seen from several applications that the calibration of Ravna & Terry

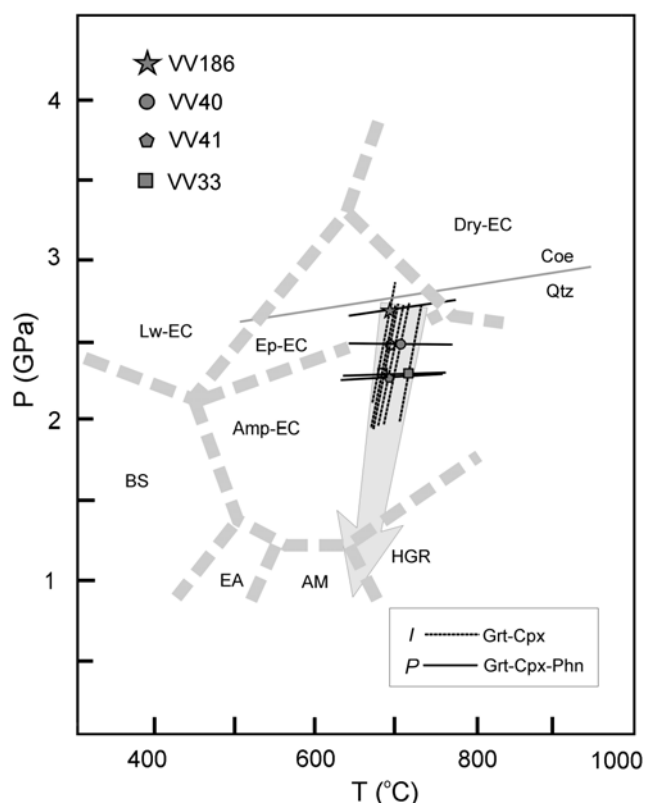


Fig. 6. Peak metamorphic P - T conditions for eclogites of the northern Veporic Unit. The post-peak decompression is shown by arrow. The metamorphic facies grid is from Okamoto & Maruyama (1999). BS — blueschist facies, EA — epidote amphibolite facies, AM — amphibolite facies, HGR — high-pressure granulite facies, Lw-EC — lawsonite eclogite facies, Ep-EC — epidote eclogite facies, Amp-EC — amphibole eclogite facies, Dry-EC — dry eclogite facies. The quartz-coesite curve is calculated from thermodynamic data of Holland & Powell (1998).

Table 5: *P-T* values for the peak metamorphic stage.

| Sample | Grt-Cpx + Grt-Cpx-Phn omphacite: stoichiometric Fe ³⁺ | | Grt-Cpx + Grt-Cpx-Phn omphacite: Fe ³⁺ = Na-(Al+Cr) |
|--------|--|--------|--|
| | P (GPa) | T (°C) | T (°C) |
| VV41 | 2.26 | 697 | 697 |
| VV40 | 2.48 | 697 | 705 |
| VV33 | 2.28 | 684 | 725 |
| VV186 | 2.72 | 692 | 692 |

(2004) gives consistent values for most HP/UHP metamorphic terrains examined. Taking into consideration all these factors, maximum *P-T* conditions for the Veporic eclogites appear to be around 2.5 GPa at 700 °C.

Discussion

The estimated *P-T* conditions together with preservation of peak assemblage Grt+Cpx I+Phn+Rt+Qtz+Zo±Amp clearly document the eclogite facies stage. If amphibole inclusions in garnet really belong to the peak-pressure assemblage is not equivocal but the experimental data would limit their stability to 2.5–2.6 GPa at 650–700 °C (e.g. Poli & Fumagalli 2003). Most of the amphibole forming the symplectites, kelyphites and matrix post-dates the peak pressure conditions. Breakdown of omphacite leads to its replacement by symplectitic intergrowths of sodic plagioclase and clinopyroxene with lower Na and Al content than the initial clinopyroxene. This is important to stress with respect to discussion on formation of such symplectites in the garnet-clinopyroxene metabasites of the Western Carpathians where omphacite has not been found (e.g. Hovorka & Méres 1989, 1990; Hovorka et al. 1992a; Janák et al. 1996, 1997; Korikovsky & Hovorka 2001; Faryad et al. 2005). Janák et al. (1996) “reconstructed” such omphacite with Jd₃₆ from the modal proportions in Cpx II — plagioclase symplectites in metabasites of the Western Tatra. These authors estimated the “minimum” *P-T* conditions of 1.5–1.6 GPa at 650–750 °C for eclogite facies stage, according to the reaction $Ab = Jd + Qtz$. As an alternative to the breakdown of omphacite, Korikovsky & Hovorka (2001) proposed that Cpx+Plg symplectites were produced by the prograde reaction from the epidote amphibolite to amphibolite facies at moderate pressure, on the basis of their observations from the Malá Fatra metabasites. Consequently, Korikovsky & Hovorka (2001) suggested that these rocks reached only the amphibolite facies conditions, without any high-pressure, eclogite facies stage.

As is generally known, many eclogites have experienced an overprint at lower pressure conditions during their exhumation. This may result in almost total decomposition of original omphacite, depending on several factors such as, maintaining of high temperature and rate of uplift, deformation and access of fluids during exhumation. In the investigated eclogites from the Veporic Unit the resulting mineral assemblage of Grt+Cpx+Pl+Qtz is the same as that found in many eclogites overprinted in

the high-pressure granulite facies conditions during their exhumation, as pointed out by O'Brien & Rötzler (2003). Therefore the eclogites of the Veporic Unit may have followed a *P-T* path from the eclogite to high-pressure granulite and amphibolite facies as illustrated in Fig. 6.

Although the timing of eclogite facies metamorphism in the Western Carpathians remains uncertain, available data from the host rocks of eclogites support its pre-Alpine age. Microprobe dating of monazite from the kyanite-bearing para- and ortho-gneisses in the northern Veporic Unit yielded two groups of ages: an older — Ordovician, ca. 470 Ma and a younger — Carboniferous, ca. 340 Ma. This is interpreted as records of pre-Variscan magmatism and Variscan metamorphism (Janák et al. 2002). Pre-Variscan magmatism in the Veporic Unit has been determined from dating of zircons as Cambrian (multi-grain method, Putiš et al. 2001) or Ordovician (single-grain method, Gaab et al. 2006a,b). In the northern Veporic Unit the zircons show metamorphic overprint in the Carboniferous (350–340 Ma) time (Putiš et al. 2001; Gaab et al. 2006b). Therefore we assume that the timing of high-pressure metamorphism of the investigated eclogites was Variscan, whereas their magmatic protoliths could be pre-Variscan, most probably Ordovician. Estimated maximum *P-T* conditions (2.5 GPa; 700 °C) suggest that eclogites were subducted to depths of about 80 km. Such metamorphic conditions were very different from those during the Alpine orogeny in the Western Carpathians. Alpine metamorphism attained a maximum of 600–620 °C at 1–1.2 GPa in the southern parts of the Veporic Unit (Janák et al. 2001), resulting from the crustal thickening during the Cretaceous time, after closure of the Meliata Ocean. However, it is not clear whether eclogites underwent their retrograde overprint during the Variscan and/or Alpine time. Published Ar-Ar data on amphiboles from the northern Veporic Unit yield mostly the pre-Alpine dates (Maluski 1993; Dallmeyer et al. 1996; Král et al. 1996) and Putiš et al. (1997) estimated the *P-T* conditions of about 500 °C at 0.8–0.9 GPa for Alpine metamorphism in this area. This implies that metamorphic evolution of eclogites in the northern Veporic Unit occurred mainly during the Variscan orogeny and their Alpine overprint was rather weak.

Conclusions

(1) The pre-Alpine basement of the Western Carpathians contains relics of a former high-pressure metamorphism. These are rarely preserved in metabasites of the northern Veporic Unit.

(2) Documentation of eclogite facies assemblage together with application of geothermobarometry allows recording the peak conditions of metamorphism, with maximum pressure and temperature of around 2.5 GPa and 700 °C. This may reflect initial subduction to depths of about 80 km. Subsequent retrogression led to breakdown of primary phases, apart from inclusions in the garnet, primary omphacite has been converted to symplectites of diopside and plagioclase.

(3) Our study supports previous indications on the existence of eclogites in the Western Carpathians. Breakdown reactions and inclusions of primary minerals are extremely informative for retrograded eclogites. Careful observations can discover high-pressure phases in potential eclogite-facies rocks. This can be essential to the elucidation of the Variscan orogenic events in the Western Carpathians.

Acknowledgments: We thank E. Krogh Ravna, S. Vrána and D. Plašienka for their helpful reviews. This work was supported by the Slovak Research and Development Agency under the contracts No. APVT-20-020002, APVT-20-016104 and APVV-51-046105, and Scientific Grant agency VEGA, Grants No. 2/6092/26 and 1/2025/05.

References

- Bezák V., Sassi F.P., Spišiak J. & Vozárová A. 1993: An outline of the metamorphic events recorded in the Western Carpathians (Slovakia). *Geol. Carpathica* 44, 6, 351–364.
- Biely A., Beňuška P., Bezák V., Bujnovský A., Halouzka R., Ivanička J., Kohút M., Klinec A., Lukáčik E., Maglay J., Miko O., Pulec M., Putiš M. & Vozár J. 1992: Geological map of the Nízke Tatry Mts. 1:50,000. *GÚDŠ*, Bratislava.
- Carswell D.A., O'Brien P.J., Wilson R.N. & Zhai M. 1997: Thermobarometry of phengite-bearing eclogites in the Dabie Mountains of central China. *J. Metamorphic Geology* 15, 239–252.
- Dallmeyer R.D., Neubauer F., Handler R., Fritz H., Müller W., Pana D. & Putiš M. 1996: Tectonothermal evolution of the internal Alps and Carpathians: Evidence from $^{40}\text{Ar}/^{39}\text{Ar}$ mineral and whole-rock data. *Eclogae Geol. Helv.* 89, 203–227.
- Faryad S.W., Ivan P. & Jacko S. 2005: Metamorphic petrology of metabasites from the Branisko and Čierna hora Mountains (Western Carpathians Slovakia). *Geol. Carpathica* 56, 3–16.
- Gaas A., Janák M., Poller U. & Todt W. 2006a: Alpine reworking of Ordovician protoliths in the Western Carpathians: Geochronological and geochemical data on the Muran Gneiss Complex, Slovakia. *Lithos* 87, 261–275.
- Gaas A.S., Poller U., Janák M. & Todt W. 2006b: Zircon U-Pb geochronology and isotopic characterization of the pre-Mesozoic basement of the Northern Veporic Unit (Central Western Carpathians, Slovakia). *Schweiz. Mineral. Petrogr. Mitt.* 85, 69–88.
- Ganguly J., Cheng W. & Tirone M. 1996: Thermodynamics of aluminosilicate garnet solid solution: new experimental data, an optimized model, and thermometric applications. *Contr. Mineral. Petrology* 126, 137–151.
- Holland T.J.B. 1990: Activities of components in omphacite solid solutions. *Contr. Mineral. Petrology* 105, 446–453.
- Holland T.J.B. & Powell R. 1998: An internally consistent thermodynamic data set for phases of petrological interest. *J. Metamorphic Geology* 16, 309–343.
- Hovorka D. & Méres Š. 1989: Relicts of high-grade metamorphites in Tatrovporic crystalline of the West Carpathians. *Miner. Slovaca* 21, 193–201 (in Slovak with English resume).
- Hovorka D. & Méres Š. 1990: Clinopyroxene-garnet metabasites from the Tribeč Mts. (Central Slovakia). *Miner. Slovaca* 22, 533–538.
- Hovorka D., Méres Š. & Caño F. 1992a: Petrology of the garnet-clinopyroxene metabasites from the Malá Fatra Mts. *Miner. Slovaca* 24, 45–52.
- Hovorka D., Méres Š. & Ivan P. 1992b: Pre-Alpine Western Carpathians Mts. basement complexes: geochemistry, petrology and geodynamic setting. *Terra Abstr., Supl. 2, Terra Nova* 4, 32.
- Hovorka D., Méres Š. & Ivan P. 1994: Pre-Alpine Western Carpathians basement complexes: lithology and geodynamic setting. *Mitt. Österr. Geol. Gesell.* 86, 33–44.
- Hovorka D., Ivan P. & Méres Š. 1997: Leptyno-amphibolite complex of the Western Carpathians: its definition, extent and genetical problems. In: Grecula P., Hovorka D. & Putiš M. (Eds.): Geological evolution of the Western Carpathians. *Miner. Slovaca, Monograph-Geocomplex*, Bratislava, 269–280.
- Hurai V., Janák M., Ludhová L., Horn R.E., Thomas R. & Majzlan J. 2000: Nitrogen-bearing fluids, brines and carbonate liquids in Variscan migmatites of the Tatra Mountains-heritage of high pressure metamorphism. *Eur. J. Mineral.* 12, 1283–1300.
- Ivan P., Hovorka D. & Méres Š. 1996: Gabbroid rocks — a newly found member of the leptyno-amphibolite complex of the Western Carpathians. *Slovak Geol. Mag.* 3–4, 199–203.
- Janák M. & Lupták B. 1997: Pressure-temperature conditions of high-grade metamorphism and migmatization in the Malá Fatra crystalline complex, the Western Carpathians. *Geol. Carpathica* 48, 287–302.
- Janák M., O'Brien P.J., Hurai V. & Reutel C. 1996: Metamorphic evolution and fluid composition of garnet-clinopyroxene amphibolites from the Tatra Mountains, Western Carpathians. *Lithos* 39, 57–79.
- Janák M., Hovorka D., Hurai V., Lupták B., Méres Š., Pitoňák P. & Spišiak J. 1997: High-pressure relics in the metabasites of the Western Carpathians pre-Alpine basement. In: Grecula P., Hovorka D. & Putiš M. (Eds.): Geological evolution of the Western Carpathians. *Miner. Slovaca, Monograph-Geocomplex*, Bratislava, 301–308.
- Janák M., Plašienka D., Frey M., Cosca M., Schmidt S.Th., Lupták B. & Méres Š. 2001: Cretaceous evolution of a metamorphic core complex, the Veporic unit, Western Carpathians (Slovakia): P-T conditions and in situ $^{40}\text{Ar}/^{39}\text{Ar}$ UV laser probe dating of metapelites. *J. Metamorphic Geology* 19, 197–216.
- Janák M., Finger F., Plašienka D., Petrik I., Humer B., Méres Š. & Lupták B. 2002: Variscan high P-T recrystallization of Ordovician granulites in the Veporic unit (Nízke Tatry Mountains, Western Carpathians): new petrological and geochronological data. *Geolines* 14, 38–39.
- Janák M., Méres Š. & Ivan P. 2003: First evidence for omphacite and eclogite facies metamorphism in the Veporic unit of the Western Carpathians. *J. Czech Geol. Soc.* 48, 1–2, 69–70.
- Klinec A. 1966: On the problems of structure and origin of the Vepor crystalline complex. *Západ. Karpaty* 6, 7–28 (in Slovak).
- Korikovsky S.P. & Hovorka D. 2001: Two types of garnet-clinopyroxene-plagioclase metabasites in the Mala Fatra Mountains crystalline complex, Western Carpathians: Metamorphic evolution, P-T conditions, symplectitic and kelyphitic textures. *Petrology* 9, 119–141.
- Korikovsky S.P., Putiš M. & Plašienka D. 1997: Cretaceous low-grade metamorphism of the Veporic and Noth-Gemic Zones: a result of collisional tectonics in the central Western Carpathians. In: Grecula P., Hovorka D. & Putiš M. (Eds.): Geological evolution of the Western Carpathians. *Miner. Slovaca, Monograph-Geocomplex*, Bratislava, 107–130.
- Kotov A.B., Miko O., Putiš M., Korikovsky S.P., Salmikova E.B., Kovach V.P., Yakovleva S.Z., Bereznaya N.G., Kráľ J. & Krist E. 1996: U-Pb dating of zircons of postorogenic acid metavolcanics: a record of Permian-Triassic taphrogeny of the Western Carpathian basement. *Geol. Carpathica* 47, 2, 73–79.
- Kráľ J., Frank W. & Bezák V. 1996: Hornblende $^{40}\text{Ar}/^{39}\text{Ar}$ spectra from the hornblende-bearing rocks of the Veporic unit. *Miner. Slovaca* 28, 501–513.
- Kretz R. 1983: Symbols for rock forming minerals. *Amer. Mineralogist* 68, 277–279.

- Krist E., Korikovsky S.P., Putiš M., Janák M. & Faryad S.W. 1992: Geology and petrology of metamorphic rocks of the Western Carpathian crystalline complexes. *Comenius University Press*, Bratislava, 1–324.
- Lupták B., Janák M., Plašienka D. & Schmidt S.Th. 2003: Alpine low-grade metamorphism in the Veporic Unit, Western Carpathians: phyllosilicates composition and crystallinity data. *Geol. Carpathica* 54, 367–375.
- Maluski H., Rajlich P. & Matte P. 1993: ^{40}Ar – ^{39}Ar dating of the Inner Carpathians Variscan basement and Alpine mylonitic overprint. *Tectonophysics* 223, 313–337.
- Méres Š., Hovorka D. & Ivan P. 1996: Gabbroids within the Veporic Unit of the Nízke Tatry Mts. (Western Carpathians). *Miner. Slovaca* 28, 1, 38–44 (in Slovak with English resume).
- Miko O. 1981: Mid-Paleozoic volcano-sedimentary Jánov grúň complex in the Veporic crystalline of the Nízke Tatry Mts. *Geol. Zbor. Geol. Carpath.* 32, 465–474 (in Russian).
- O'Brien P.J. & Rötzler J. 2003: High-pressure granulites: formation, recovery of peak conditions and implications for tectonics. *J. Metamorphic Geology* 21, 3–20.
- Okamoto K. & Maruyama S. 1999: The high-pressure synthesis of lawsonite in the MORB+H₂O system. *Amer. Mineralogist* 84, 362–373.
- Plašienka D., Grecula P., Putiš M., Hovorka D. & Kováč M. 1997: Evolution and structure of the Western Carpathians: an overview. In: Grecula P., Hovorka D. & Putiš M. (Eds.): Geological evolution of the Western Carpathians. *Miner. Slovaca, Monograph–Geocomplex*, Bratislava, 1–24.
- Poli S. & Fumagalli P. 2003: Mineral assemblages in ultrahigh pressure metamorphism: A review of experimentally determined phase diagrams. *EMU Notes in Mineralogy*. Vol. 5, Chapt. 10, 307–340.
- Putiš M., Filová I., Korikovsky S.P., Kotov A.B. & Madarás J. 1997: Layered metagneous complex of the Veporic basement with features of the Variscan and Alpine thrust tectonics (the Western Carpathians). In: Grecula P., Hovorka D. & Putiš M. (Eds.): Geological evolution of the Western Carpathians. *Miner. Slovaca, Monograph–Geocomplex*, Bratislava, 176–196.
- Putiš M., Kotov A.B., Korikovsky S.P., Sahnikova E.B., Yakovleva S.Z., Berezhnaya N.G., Kovach V.P. & Plotkina J.V. 2001: U/Pb zircon ages of dioritic and trondhjemitic rocks from a layered amphibolitic complex crosscut by granite vein (Veporic basement, Western Carpathians). *Geol. Carpathica* 52, 49–60.
- Ravna E.J.K. 2000: The garnet-clinopyroxene Fe²⁺–Mg geothermometer: An updated calibration, *J. Metamorphic Geology* 18, 211–219.
- Ravna E.J.K. & Paquin J. 2003: Thermobarometric methodologies applicable to eclogites and garnet ultrabasites. *EMU Notes in Mineralogy*, Vol. 5, Chapt. 8, 229–259.
- Ravna E.J.K. & Terry M.P. 2004: Geothermobarometry of UHP and HP eclogites and schists — an evaluation of equilibria among garnet-clinopyroxene-kyanite-phengite-coesite/quartz. *J. Metamorphic Geology* 22, 579–592.
- Spišiák J. & Pitoňák P. 1990: Nízke Tatry Mts. crystalline complex — new facts and interpretation (Western Carpathians, Czechoslovakia). *Geol. Zbor. Geol. Carpath.* 41, 377–392.
- Vrána S. 1966: Alpidische Metamorphose der Granitoide und Foederata-Serie im Mittelteil der Veporiden. *Zbor. Geol. Vied, Západ. Karpaty* 6, 29–84.
- Waters D.J. & Martin H.N. 1993: Geobarometry of phengite-bearing eclogites. *Terra Abstracts* 5, 410–411.
- Waters D.J. & Martin H.N. 1996: The Garnet-Cpx-Phengite barometer. Recommended calibration and calculation method, updated 1st March 1996. <http://www.earth.ox.ac.uk/davewa/research/eclogites/ecbarca.html>.